Structure analysis of a phenylpyrazole carboxylic acid derivative crystallizing with three molecules in the asymmetric unit ($Z' = 3$) using X-ray powder diffraction

S. Ghosh,[1] S. Pramanik,[2,3] and A. K. Mukherjee[2,a)]
[1]*Department of Physics, Chakdaha College, Chakdaha, Nadia, West Bengal, Pin-741222, India*
[2]*Department of Physics, Jadavpur University, Kolkata-700032, India*
[3]*Department of Physics, Dinabandhu Mahavidyalaya (Bongaon), Bangaon, West Bengal, Pin-743235, India*

(Received 4 December 2018; accepted 26 February 2019)

Crystal structure analysis of a pyrazole carboxylic acid derivative, 5-(trifluoromethyl)-1-phenyl-1H-pyrazole-4-carboxylic acid (**1**) has been carried out from laboratory powder X-ray diffraction data. The crystal packing in the pyrazole carboxylic acid derivative exhibits an interplay of strong O–H. . .O, C–H. . .N and C–H. . .F hydrogen bonds to generate a three-dimensional molecular packing via the formation of $R_2^2(8)$ and $R_2^2(9)$ rings. Molecular electrostatic potential calculations indicated that carbonyl oxygen, pyrazole nitrogen and fluorine atoms to be the strongest acceptors. The relative contribution of different interactions to the Hirshfeld surface of pyrazole carboxylic acid and a few related structures retrieved from CSD indicates that H. . .H, N. . .H and O. . .H interactions can account for almost 70% of the Hirsfeld surface area in these compounds. © *2019 International Centre for Diffraction Data*. [doi:10.1017/S0885715619000289]

Key words: X-ray powder diffraction, Hirshfeld surface analysis, crystal structure determination

I. INTRODUCTION

In recent years, there has been growing interest in crystal structures with $Z' > 1$ (Hao *et al*., 2005a, 2005b; Lehmler *et al*., 2004; Desiraju, 2007; Bernstein *et al*., 2008; Johnstone *et al*., 2010; Bernstein, 2011; Steed and Steed, 2015; Brock, 2016). The underlying causes of how and why some crystal structures have high Z' values are still not completely understood. One hypothesis is that crystal structures with $Z' > 1$ are meta-stable forms of thermodynamically stable $Z' = 1$ polymorph (Anderson and Steed, 2007) and the molecules assemble into clusters prior to reaching the highest symmetry arrangements (Das *et al*., 2006; Lodochnikova *et al*., 2014). It has been generally accepted that in addition to causes like modulation, equi-energetic conformations, crystallization kinetics etc, structures with $Z' > 1$ are consequence of conflict between different factors influencing the crystal packing, space group constraints and intermolecular interactions (Hao *et al*., 2005a; 2005b; Nichol and Clegg, 2006; Owczarzak *et al*., 2013; Das *et al*., 2016). Steed and coworkers (Anderson *et al*., 2011) on the basis of an exhaustive CSD (Allen and Taylor, 2004) analysis concluded that structures with $Z' > 1$ are linked to molecular shapes that can frustrate or impose some constraints on their crystal packing arrangements.

In general, single crystal X-ray diffraction is the method of choice for determining crystal structures of molecular compounds. An intrinsic limitation of this approach is, however, the requirement to grow single crystals of appropriate size and quality that make them amenable to structure analysis. With the recent advances in X-ray powder diffraction instrumentation coupled with the developments in direct space approaches for structure solution (Pagola *et al*., 2000; Harris and Cheung, 2004; Favre-Nicolin and Cerný, 2004; David and Shankland, 2008), ab-initio crystal structure analysis of molecular compounds using powder X-ray diffraction (PXRD) has become a viable alternative in structural crystallography (Arlin *et al*., 2014; Watts *et al*., 2016; Chatterjee *et al*., 2017; Pramanik *et al*., 2019). It should, however, be emphasized that structure analysis from PXRD is significantly more challenging than that of its single-crystal counterpart (Harris *et al*., 2001) and the task of ab-initio structure determination via PXRD is far more difficult when the molecule possesses considerable flexibility or the asymmetric unit contains multiple molecules ($Z' > 1$). This is reflected from the CSD (Version 5.39 November CSD 2018 release) (Allen and Taylor, 2004) search conducted for organic structures with $Z' > 1$, which revealed that out of 50 215 hits, structures of 160 (0.3%) have been solved from powder diffraction data. If we restrict our search to organic compounds crystallizing with $Z' = 3$, the number of structures solved via powder diffraction approach is only 13, the corresponding number with single crystal diffraction is 2662. Out of 13 structures with $Z' = 3$ that have been solved using powder diffraction method, crystal structures of only two compounds (Platteau *et al*., 2005; Martin *et al*., 2016) have been determined using laboratory PXRD data; the remaining 11 structures have been solved using either synchroton X-ray or neutron diffraction data.

In continuation to our ongoing study of structure analysis of benzoic acid derivatives (Pramanik *et al*., 2019) using PXRD and the role of weak intermolecular interactions in building supramolecular assembly, we came across the title compound,

a)Author to whom correspondence should be addressed. Electronic mail: akm_ju@rediffmail.com

5-(trifluoromethyl)-1-phenyl-1H-pyrazole-4-carboxylic acid (**1**), which crystallized with $Z' = 3$. Since there are only two reports of structure analysis of molecular compounds crystallizing with $Z' = 3$, the present work was undertaken. An investigation of close intermolecular contacts via Hirshfeld surface analysis of different molecules in the asymmetric unit of **1** and a few related structures is also presented. The intermolecular interactions in **1** have been correlated with the molecular electrostatic potential (MEP) calculations.

II. EXPERIMENTAL

A. Materials and methods

The compound, 5-(trifluoromethyl)-1-phenyl-1H-pyrazole-4-carboxylic acid (**1**) was purchased from Sigma Aldrich, NY, USA and used without further purification. PXRD data of compound **1** were collected at ambient temperature [293(2) K] with Cu$K\alpha$ radiation ($\lambda = 1.5418$ Å) using a Bruker D8 Advance diffractometer operating in the Bragg-Brentano geometry.

B. Crystal structure determination using PXRD

Initially, the indexing of PXRD pattern of the title compound (**1**) using conventional method i.e. extraction of 2θ positions of first 25 peaks and input those peak positions in the indexing program TREOR (Werner *et al*., 1985) was unsuccessful. Ultimately the program package EXPO-2004 (Altomare *et al*., 2013) was used for successful determination of unit cell parameters. The auto peak search method of EXPO-2014 (Altomare *et al*., 2013) shows an unresolved peak at 5.27° (2θ). The inclusion of the unresolved peak at 5.27° (2θ) along with the extracted 2θ-positions of rest of the peaks in the auto-indexing module of NTREOR (Altomare *et al*., 2000) as implemented in the EXPO 2014 (Altomare *et al*., 2013) program package lead to a successful indexing. Given the volume of the triclinic unit cell and consideration of density of related carboxylic acid compounds, the number of formula units in the unit cell of **1** turned out to be 6. The unit cell parameters and space group assignment were validated by a Le-Bail fit of PXRD data using a pseudo-Voigt peak profile function (Thompson *et al*., 1987) with program FOX (Favre-Nicolin and Cerný, 2004). Structure solution of **1** was carried out by global optimization of structural models in direct space, based on a Monte-Carlo search using the simulated annealing technique (in parallel tempering mode), as implemented in FOX (Favre-Nicolin and Cerný, 2004). Initial molecular geometry input in FOX was optimized with MOPAC 9.0 (Stewart, 2007) using the energy gradient method.

The best solution (i.e. the structure with the lowest R_{wp} value and no unusual short contacts) was used as the initial structural model of **1** for Rietveld refinement (Rietveld, 1967) with GSAS program (Larson and Von Dreele, 2000). A pseudo- Voigt peak profile function was used during Rietveld refinement and the background of PXRD patterns was modeled by a shifted Chebyshev function of the first kind with 10 points regularly distributed over the entire 2θ range. Initially, the lattice parameters, background coefficients and profile parameters were refined followed by the positional coordinates of all non-hydrogen atoms. Soft distance and angle restraints with weight value 10 for bond-distances and bond-angles were applied. The probable bond distances and angles for restraints were chosen from the CSD search (Allen and Taylor, 2004). Planar restraints were used for the phenyl rings with weight value of 20. Common isotropic displacement parameters were refined separately for C, O, N, and F atoms. In the final stages of refinement, preferred orientation parameters were refined using the generalized spherical harmonics model, and the order of spherical harmonics used to describe the preferred orientation was 6. Final Rietveld plot of **1** (Figure 1) showed good agreement between the observed PXRD profile and calculated PXRD pattern. A summary of crystal data and relevant refinement parameters is listed in Table I.

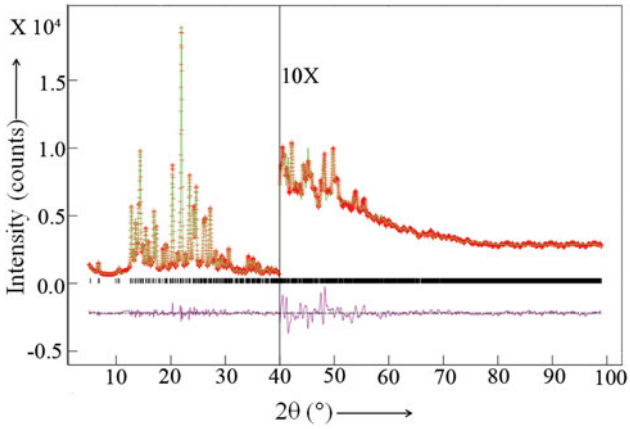

Figure 1. (Color online) Final Rietveld plot of $C_{11}H_7F_3N_2O_2$ (**1**), Observed pattern (red cross), calculated pattern (green curve), difference curve (pink curve): The intensity in the high angle region has been multiplied by a factor 10.

C. Hirshfeld surface analysis

Hirshfeld surfaces (McKinnon *et al*., 2007) and their associated two-dimensional (2D) fingerprint plots (Spackman and McKinnon, 2002) were generated using Crystal Explorer 3.1

TABLE I. Crystal data and structure refinement parameters for $C_{11}H_7F_3N_2O_2$ (**1**).

Formula weight	256.18
Temperature(K)	293(2)
Crystal system	Triclinic
Space group, Z	P-1, 6
Wavelength(Å)	1.54056 (Cu$K\alpha_1$) & 1.54443 (Cu$K\alpha_2$)
a (Å)	18.1701(18)
b (Å)	14.1169(7)
c (Å)	7.0817(6)
α (°)	96.4733(31)
β (°)	99.847(7)
γ (°)	68.519(5)
Volume(Å^3)	1648.14(24)
Density(calculated) g cm^{-3}	1.549
2θ interval(°)	$5 < 2\theta < 100$
Step size(°)	0.02
R_p	0.0440
R_{wp}	0.0580
R_F^2	0.1103
χ^2	4.709

https://doi.org/10.1017/S0885715619000289 Published online by Cambridge University Press

(Wolff *et al*., 2012) software. The d_{norm} (normalized contact distance) surface, 2D fingerprint plot and that delineated into individual contacts were used for decoding and quantifying intermolecular interactions in the crystal lattice of **1**. The d_{norm} is a symmetric function of distances to the surfaces from nuclei inside and outside the Hirshfeld surface (d_i and d_e, respectively), relative to their respective van-der-Waals (vdW) radii. A color scale of red (shorter than vdW separation), white (equal to vdW separation) and blue (longer than vdW separation) was used to visualize the intermolecular contacts. The 3D d_{norm} surfaces were mapped over a fixed color scale of −0.22 (red) to 1.40 Å (blue). The 2D fingerprint plots of **1** were displayed by using the translated 0.5–2.5 Å range and including reciprocal contacts.

D. Computational study

MEP is an effective tool for identifying and ranking the hydrogen bond donating and accepting sites in organic compounds (Aakeröy *et al*., 2015; Politzer and Murray, 2015). Density functional theory (DFT) calculations were performed in the solid state (periodic) for compound **1** with the DMol^3 code (Delley, 1990) in the framework of a generalized gradient approximation (GGA) (Perdew *et al*., 1996). The geometry optimization was carried out using BLYP correlation functional (Becke, 1988; Lee *et al*., 1988) with a double numeric plus polarization (DNP) basis set. The starting atomic coordinates were taken from the final X-ray refinement cycle, and geometry optimization was carried out without any structural constraints. The MEP surfaces of **1** were generated, and the electron densities were evaluated using an isolated molecule DFT calculation starting with the geometry optimized models as input in the DMol^3 code with the same set up as earlier. The electrostatic potentials were plotted on 0.017 au electron density isosurface (Bader *et al*., 1987). The MEP surfaces were mapped with a rainbow color scheme with red representing the highest negative potential region while blue represents the highest positive potential region.

III. RESULT AND DISCUSSIONS

A. Structure description

The molecule **1** consists of phenyl pyrazole carboxylic acid fragment with a trifluromethyl group substitution at the 5-position of central pyrazole ring (Scheme 1). The conformation of molecules in **1** is established by the rotational degree of freedom around the N–C bond connecting the pyrazole and benzene rings. A view of asymmetric unit of **1** containing three symmetry-independent molecules (A, B, and C) with the atom labeling scheme is shown in Figure 2. The molecules do not differ significantly in terms of geometrical parameters. An overlay of three molecules (A, B, and C) in the asymmetric unit of **1** is shown in Figure 3. The overall conformation of molecules A, B, and C can be described by the relative orientation of two planar fragments, phenyl ring (P: C1-C6 atoms) and the pyrazole moiety (Q: N1/N2/C7-C9 atoms). The dihedral angles between the least-squares planes through atoms of rings P and Q in molecules A, B, and C are 47.4(3), 48.7(3), and 60.7(4)°, respectively. The twist between rings P and Q about the C6-N1 bond differs significantly for molecules A, B, and C; the corresponding torsion angle C1-C6-N1-C9 for molecules A, B, and C is 146.0(7), −144.7(7), and −70.2(6)°, respectively (Table S1). As revealed by the torsion angle C7-C8-C10-O1 of −2.0(1), 174.7(9) and −167.5(9)° for molecules A, B, and C, the orientation of carboxylic acid group (C10,O1,O2,H2) in A differs from that of B and C because of rotation about the C8-C10 bond.

The bond lengths and bond angles of the phenylpyrazole core are comparable with those reported for similar compounds (Antila *et al*., 2004; Rehman *et al*., 2008; Caruso *et al*., 2009; Wen *et al*., 2015). A MOGUL analysis of pyrazole derivatives indicates that the range of N–N distance lies between 1.210 and 1.458 Å and the observed N1-N2 bond length [1.255(6)–1.267(6) Å] in **1** is within this range. The shortening of C8-C10 bond length [1.371(6)–1.392(6) Å] in **1** is probably a consequence of π-delocalization of adjacent C8-C9 and C10-O1 double bonds. A similar MOGUL search shows that C7-N2-N1 bond angle [110.3(4)-111.7(5)°] lies within the range of C–N–N angle of [110.3°–113.1°] with a mean value of 111.6°. A superposition of molecular conformations of **1** as determined by the X-ray structure analysis and solid-state DFT calculations is shown in Figure S1. The energies of three molecular conformations of **1** (A, B, and C) as determined by isolated molecule DFT calculation are essentially similar i.e. −122.0 eV, −121.5 eV, and −121.8 eV for molecules A, B, and C, respectively.

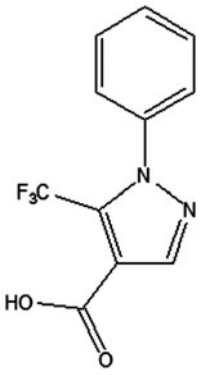

Scheme 1. Chemical diagram of $C_{11}H_7F_3N_2O_2$ (1).

B. Crystal packing analysis

The molecules B and C in **1** are linked with themselves through pairs of intermolecular O2(B)-H2(B)...O1(B) and O2(C)-H2(C)...O1(C) hydrogen bonds (Table II) to form a typical carboxylic acid dimer with an $R_2^2(8)$ synthon (Figure S2). The molecule A, however, does not facilitate such dimer formation. Similarly, the intermolecular O2(A)-H2(A)...N2(B) and C1(B)-H1(B)...O1(A) hydrogen bonds connect molecules A and B into a cyclic $R_2^2(9)$ ring. The $R_2^2(8)$ and $R_2^2(9)$ rings are further joined by intermolecular C2(C)-H2(C)...F2(A) hydrogen bond, thus generating an infinite 1D chain of sequence...ABBACCA...(Figure S2). Adjacent polymeric chains are connected by intermolecular C7(C)-H7(C)....F2(B) hydrogen bond forming a 2D framework in the (011) plane (Figure 4). Finally, linking of parallel 2D molecular sheets via intermolecular C5(C)-H5(C)...F3(C) hydrogen bond results into a 3D architecture in **1**.

https://doi.org/10.1017/S0885715619000289 Published online by Cambridge University Press

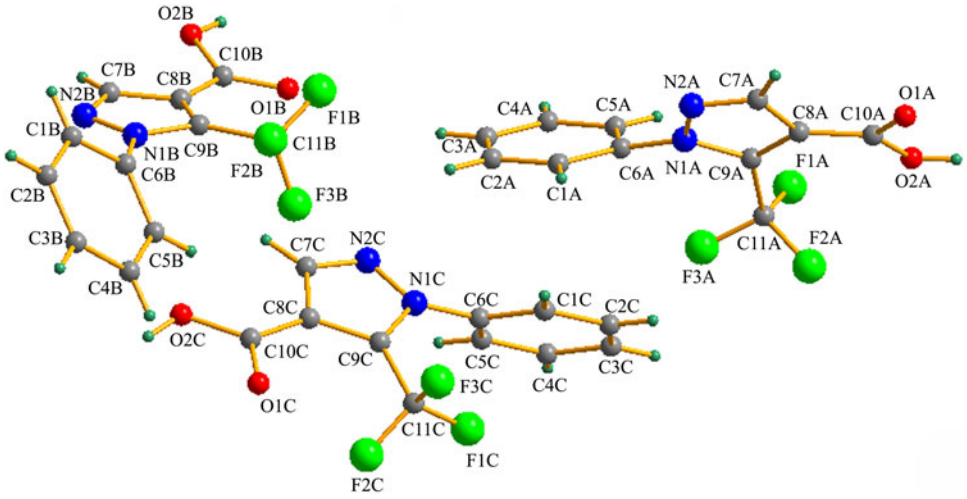

Figure 2. (Color online) Molecular view with the atom labeling scheme of $C_{11}H_7F_3N_2O_2$ (**1**).

C. Hirshfeld surface analysis

The Hirshfeld surfaces for different molecules in the asymmetric unit of **1** are illustrated in Figure 5, showing surfaces that have been mapped over a d_{norm} range of −0.5 Å to 1.5 Å. Since Hirshfeld surface is related to a given molecular environment, it can enable a rapid and easy visualization of interactions encountered by independent molecules in the asymmetric unit of structures with $Z' > 1$ (Anderson *et al*., 2006; Rohl *et al*., 2008). The dominant interaction between the carboxylic O–H and O atoms of molecule C can be seen in the Hirshfeld surface as bright red spots marked as *c/c*' in Figure 5(c). The light red spots labeled as a/a' in Figure 5(a) and b/b' in Figure 5(b) are because of O2(A)-H2(A)...N2(B)/ C1(B)-H1(B)...O1(A) and O2(B)-H2(B)...O1(B) interactions experienced by molecules A and B. Other visible red areas in the Hirshfeld surfaces (Figure 5) are attributable to C–H...F contacts in **1**. The corresponding 2D fingerprint plots of **1** (Figure 5) and that delineated into individual contact types (Figure 5) are distinctly different for molecules A, B, and C indicating a difference in their intermolecular interactions. Two sharp spikes (c/c' in Figure 5(l)) of almost equal lengths in the region of $1.4 < d_e + d_i < 1.5$ Å are characteristic of O–H...O hydrogen-bonded cyclic $R_2^2(8)$ ring formed by molecule C. The spikes corresponding to N–H interactions in molecules A and B are highly asymmetric (Figures 5(s) and 5(t)). In molecule A, the donor spike (a in Figure 5(s)) because of O2(A)-H2(A)...N2(B) interaction is significantly longer compared to the acceptor spike (a' in Figure 5(s)) because of N2(A)...H4(A)-C4(A) interaction. In molecule B, however, the length of the acceptor spike (e' in Figure 5(t)) because of N2(B)...H2(A)-O2(A) interaction is more compared to the donor spike of C7(B)-H7(B)...N2(A) interaction (e in Figure 5(t)). The asymmetry in the length of spikes can be attributed to the variation of H...N distances between molecules A...A and A...B (2.01–2.77 Å) and B...A (2.01–2.96 Å). The subtle difference among the fingerprint plots for molecules A, B, and C is also apparent in terms of F...H and H...H interactions (Figure 5), which is reflected in the corresponding spikes for the F...H contacts and distribution of scattered points because of H...H interactions.

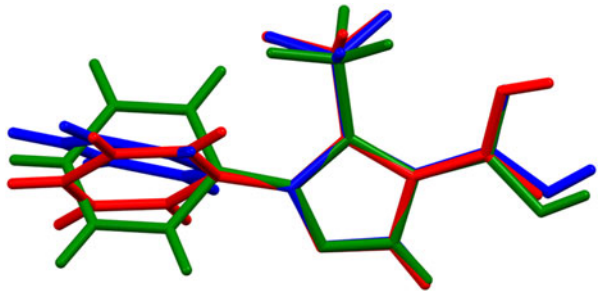

Figure 3. Overlay of three molecules [A (red), B (green) and C (blue)] in asymmetric unit of $C_{11}H_7F_3N_2O_2$ (**1**).

The enrichment ratio (E) (Jelsch *et al*., 2014), defined as the ratio of proportion of actual contacts in the crystal to the theoretical proportion of random contacts, has been calculated for molecules A, B and C of **1**. For pair of elements with higher propensity to form contacts, the calculated *E* is greater than unity; while pairs of elements, which tend to avoid contacts yield *E* values less than unity (Jelsch *et al*., 2014). The E_{HN} values for molecules A, B and C are 1.62, 1.42, and 1.44, respectively, which indicate that H...N contacts are favored in all three molecules (A, B and C) of the asymmetric unit of **1**. A similar trend has been observed for H...O contacts in molecules A, B, and C with E_{HO} values of 1.25, 1.38, and 1.50, respectively. An increased propensity of H...C contacts to form has been observed only in molecule C ($E_{HC} = 1.10$), the corresponding E_{HC} values for molecules A and B are 0.78 and 0.65, respectively. This can be rationalized following the higher percentage of H...C contacts to the total Hirshfeld surface area of **1** for molecule C (16.1%) compared to that in A (10.3%) and B (9.3%). Fluorine atom behaves somewhat differently from the other halogen atoms (Cl, Br, and I) because of its small size, weak polarizability, higher electronegativity, and strong electron-withdrawing ability. The role of H...F and O...F interactions in the crystal packing of organic compounds has been reviewed recently (Berger *et al*., 2011). The E_{HF} values of 1.34, 1.13, and 1.34, respectively, for molecules A, B, and C of **1** indicate an increased propensity of formation of H...F contacts. The O...F contacts are, however, favored in molecules A and B with E_{OF} values of 1.17 and 1.07, respectively, while that in molecule C are highly

https://doi.org/10.1017/S0885715619000289 Published online by Cambridge University Press

TABLE II. Intermolecular C–H..O, O–H. . .N, C–H. . .F, C–H. . .π hydrogen bonds and C–F. . .O halogen bond in compound $C_{11}H_7F_3N_2O_2$ (**1**).

Interactions	D–H (Å)	H. . .A (Å)	D. . .A (Å)	D–H. . ..A (°)	Symmetry
O2C–H2C1. . .O1C	0.83	1.71	2.5401(3)	170	-*x*, -*y*, 1-*z*
O2A–H2A1. . .N2B	0.83	2.03	2.8317(3)	160	1-*x*, 1-*y*,1-*z*
C5C–H5C. . .F3C	0.93	2.29	3.1374(3)	151	*x*, *y*, 1 + *z*
O2B–H2B1. . .O1B	0.83	2.44	3.2564(3)	168	-;*x*, 1-*y*, -*z*
C1B–H1B. . .O1A	0.93	2.59	3.3109(3)	134	1-*x*, 1-*y*, 1-*z*
C2C–H2C. . .F2A	0.93	2.51	3.2527(3)	137	*x*, *y*, 1 + *z*
C7C–H7C. . .F2B	0.93	2.60	3.4391(3)	149	2-*x*, 2-*y*, -*z*

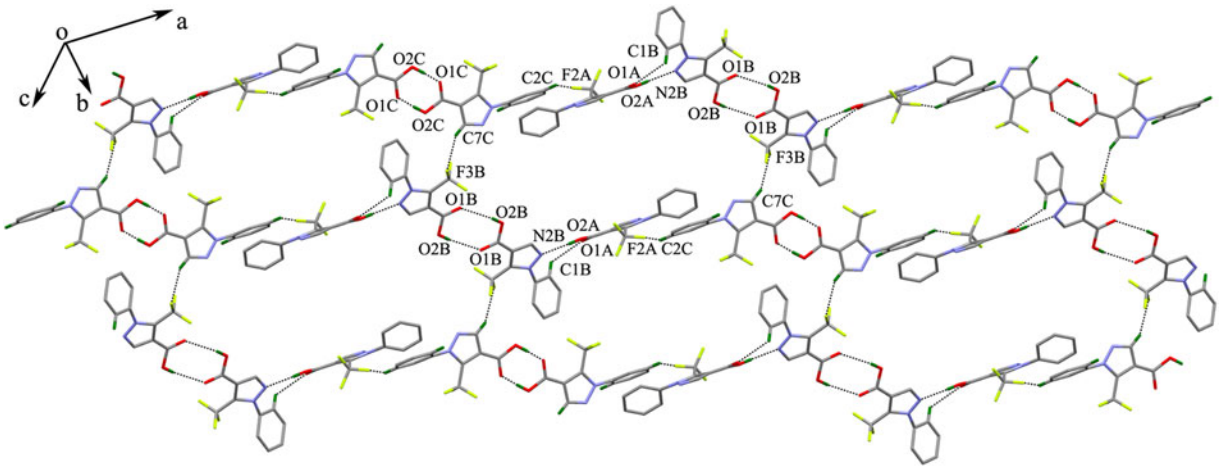

Figure 4. (Color online) 2D molecular framework formed by C–H. . .O, C–H. . .N and O–H. . .N hydrogen bonds in $C_{11}H_7F_3N_2O_2$ (**1**).

disfavored ($E_{OF} = 0.37$). The apparent discrepancy in the E_{OF} values for three symmetry-independent molecules in the asymmetry unit of **1** is a consequence of the fact that only molecules A and B (not C) are involved in C–F. . .O interactions (Table II).

The relative contribution of different interactions to the Hirshfeld surface of **1** for molecules A, B, and C, and a few related carboxylic acid/carboxylate derivatives such as, 5-chloro-3-methyl-1-phenyl-1H-pyrazole-4-carboxylic acid (FUJTOV) (Wen *et al.*, 2015), 5-amino-3-(trifluoromethyl)-1-phenyl-1H-Pyrazole-4-carboxylic acid (HUDDEQ) (Caruso *et al.*, 2009), 5-amino-1-phenyl-1H-pyrazole-4-carboxylic acid (KODXIL) (Rehman *et al.*, 2008) and ethyl 3-(trifluoromethyl)-1-phenyl-1H-pyrazole-4-carboxylate (WADVED) (Antila *et al.*, 2004), retrieved from the CSD (Version 5.39 November CSD 2018 release) is illustrated in Figure 6. The contribution of F. . .H interaction to the Hirshfeld surface of **1** is highest (32.0%) for molecule C, whereas the contribution of H. . .N and H. . .O interactions are maximum for molecules A and B, respectively. An enhanced contribution of H. . .C interactions to the Hirshfeld surface of **1** for molecule C (16.1%) compared to that in molecules A and B (9.2–10.3%) is expected since the phenyl ring of only molecule C participates in C–H. . .π interaction. The compound **1** bears a close structural resemblance with ethyl 3-(trifluoromethyl)-1-phenyl-1H-pyrazole-4-carboxylate (WADVED). With a change in the position of trifluoromethyl group substitution in pyrazole ring and the hydroxyl group in **1** being replaced by a ethyl group in WADVED, the contribution of H. . .H interactions to the Hirshfeld surface increases from 17.1- 20.7% in **1** to 30.1% in WADVED.

D. Molecular electrostatic potential

The MEP surfaces were calculated for molecules A, B, and C to validate the hydrogen bonding patterns in **1** (Figure S3). The MEP values around different atoms can serve as a good indicator of possible donor and acceptor sites in a molecule. In **1**, the most positive potential ($V_{s,max}$ 74–75 kcal/mol) is linked with the hydrogen atom (H2) of the carboxylic group in molecules A, B and C. The corresponding most negative potentials ($V_{s,min}$) of −35 to −42 Kcal/mol are associated with the carbonyl oxygen atom of the COOH group. Crystallographic analysis of **1** also corroborates this as intermolecular O–H. . .O, O–H. . .N and C–H. . .O hydrogen bonds involving molecules A, B and C form $R_2^2(8)$ and $R_2^2(9)$ synthons. Relatively high positive potentials surrounding the hydrogen atoms (H1-H5, H7) of the aromatic rings and negative potentials around the pyrazole nitrogen atom (N2) in molecules A, B, and C are attributable to intra/ intermolecular interactions involving these atoms.

IV. CONCLUSIONS

Crystal structure analysis of a trifluoromethyl derivative of phenyl trizole carboxylic acid (**1**) crystallizing with three molecules (A, B, and C) in the asymmetric unit has been carried out using laboratory PXRD data. The relative orientation between the phenyl and pyrazole rings in **1** is different for molecules A, B, and C because of rotation about the C–N bond connecting the two aromatic fragments. Significant changes in the intermolecular interactions experienced by molecules A, B and C have been observed. While the

https://doi.org/10.1017/S0885715619000289 Published online by Cambridge University Press

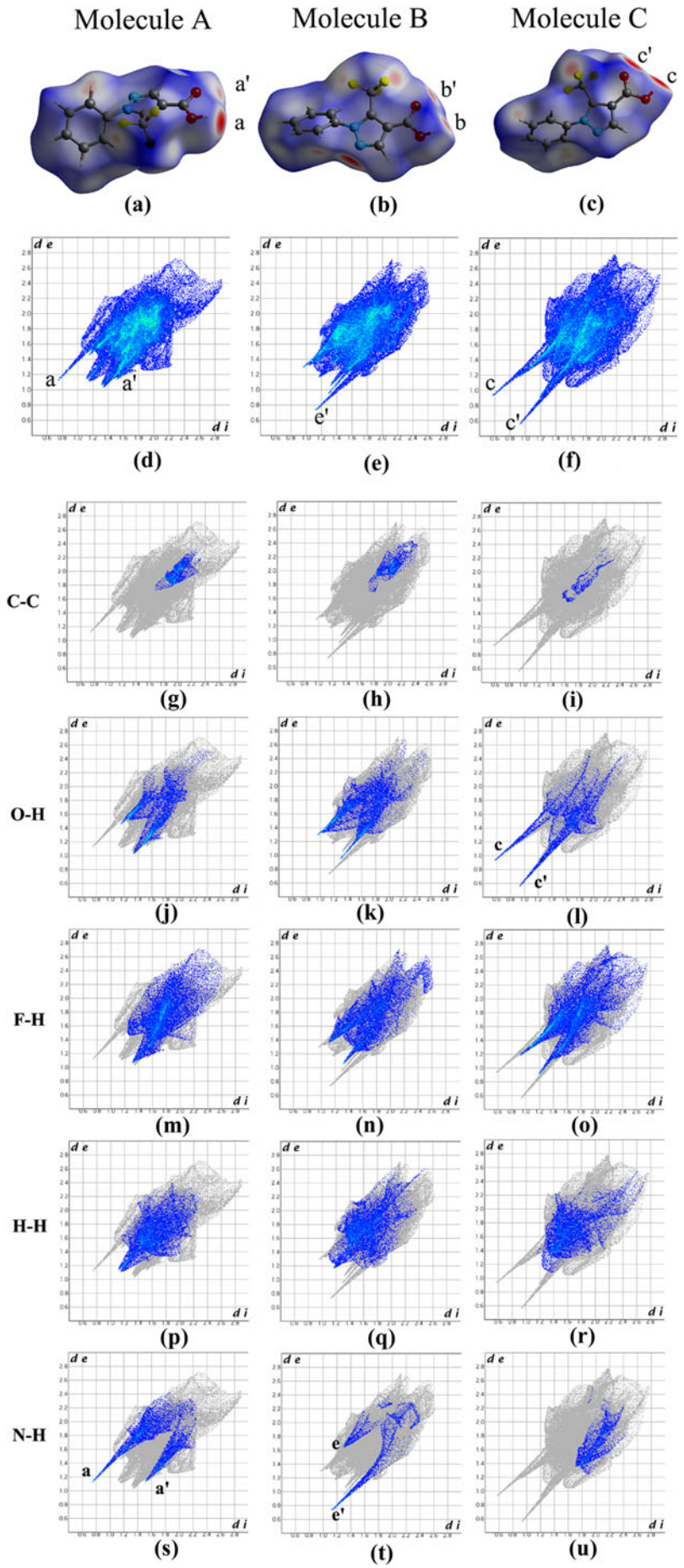

Figure 5. (Color online) Hirshfeld surface and 2D fingerprint plots of $C_{11}H_7F_3N_2O_2$ (**1**).

https://doi.org/10.1017/S0885715619000289 Published online by Cambridge University Press

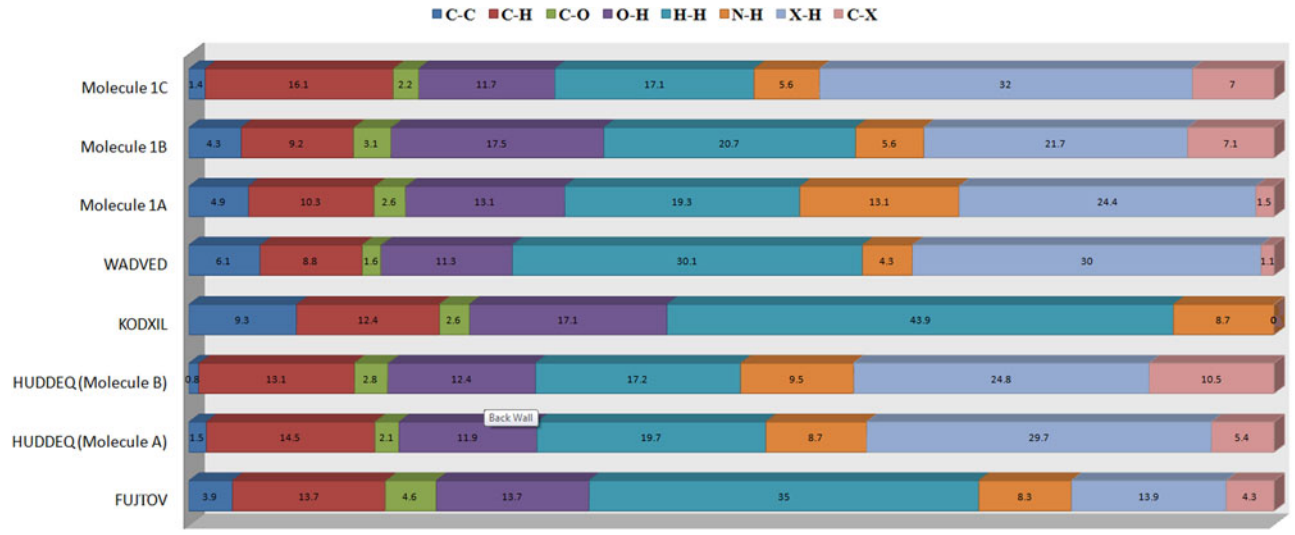

Figure 6. (Color online) Relative contribution of different interactions to Hirshfeld surface of $C_{11}H_7F_3N_2O_2$ (**1**) and a few related structures retrieved from the CSD.

hydroxyl and the oxo groups of carboxylic moieties in molecules B and C form an $R_2^2(8)$ homosynthon via intermolecular O–H. . .O hydrogen bond, the molecule A participates in intermolecular O–H. . .N and C–H. . .O hydrogen bonds with molecule B to generate an $R_2^2(9)$ heterosynthon. The resulting pattern can be described by infinite 1D chains of sequence. . .. ABBACCA. . ., which are interconnected forming a 3D framework structure in **1**. The study clearly demonstrates the potential of laboratory PXRD to solve crystal structure of systems crystallizing with multiple molecules in the asymmetry unit ($Z' > 1$). To the best of our knowledge, there are only two earlier reports of successful crystal structure analysis of molecular compounds with $Z' = 3$ using laboratory PXRD data.

SUPPLEMENTARY MATERIAL

The supplementary material for this article can be found at https://doi.org/10.1017/S0885715619000289

ACKNOWLEDGEMENT

Financial support from University Grants Commission (UGC), New Delhi, India to SG through grant no. F. PSW-089/13-14 dated 18-March-2014, is acknowledged.

Aakeröy, C. B., Wijethunga, T. K., and Desper, J. (**2015**). "Molecular electrostatic potential dependent selectivity of hydrogen bonding," New J. Chem. **39**, 822–828.

Allen, F. H., and Taylor, R. (**2004**). "Research applications of the Cambridge Structural Database (CSD)," Chem Soc Rev. **33**, 463–475.

Altomare, A., Giacovazzo, C., Guagliardi, A., Moliterni, A. G. G., Rizzi, R., and Werner, P.-E. (**2000**). "New techniques for indexing: n-TREOR in EXPO," J. Appl. Crystallogr. **33**, 1180–1186.

Altomare, A., Cuocci, C., Giacovazzo, C., Moliterni, A., Rizzi, R., Corriero, N., and Falcicchio, A. (**2013**). "*EXPO*2013: a kit of tools for phasing crystal structures from powder data," J. Appl. Crystallogr. **46**, 1231–1235.

Anderson, K. M., and Steed, J. W. (**2007**). "Comment on "On the presence of multiple molecules in the crystal asymmetric unit ($Z' > 1$) by Gautam R. Desiraju," CrystEngComm. **9**, 328–330.

Anderson, K. M., Afarinkia, K., Yu, H.-W., Goeta, A. E., and Steed, J. W. (**2006**). "When $Z' = 2$ is better than $Z = 1$ supramolecular centrosymmetric hydrogen-bonded dimers in chiral systems," Cryst. Growth Des. **6**, 2109–2113.

Anderson, K. M., Probert, M. R., Goeta, A. E., and Steed, J. W. (**2011**). "Size does matter—the contribution of molecular volume, shape and flexibility to the formation of co-crystals and structures with $Z' > 1$," CrystEngComm. **13**, 83–87.

Antila, J. C., Baskin, J. M., Barder, T. E., and Buchwald, S. L. (**2004**). "Copper−Diamine-Catalyzed *N*-arylation of pyrroles, pyrazoles, indazoles, imidazoles, and triazoles," J. Org. Chem. **69**, 5578–5587.

Arlin, J. B., Bhardwaj, R. M., Johnston, A., Miller, G. J., Bardin, J., MacDougall, F., Fernandes, P., Shankland, K., David, W. I. F., and Florence, A. J. (**2014**). "Structure and stability of two polymorphs of creatine and its monohydrate," CrystEngComm. **16**, 8197–8204.

Bader, R. F. W., Carroll, M. T., Cheeseman, J. R., and Chang, C. (**1987**). "Properties of atoms in molecules: atomic volumes," J. Am. Chem. Soc. **109**, 7968–7979.

Becke, A. D. (**1988**). "Density-functional exchange-energy approximation with correct asymptotic behaviour," Phys. Rev. A. **38**, 3098–3100.

Berger, R., Resnati, G., Metrangolo, P., Weber, E., and Hulliger, J. (**2011**). "Organic fluorine compounds: a great opportunity for enhanced materials properties," Chem. Soc. Rev. **40**, 3496–3508.

Bernstein, J. (**2011**). "Polymorphism−A perspective," Cryst. Growth Des. **11**, 632–650.

Bernstein, J., Dunitz, J. D., and Gavezzotti, A. (**2008**). "Polymorphic perversity: crystal structures with many symmetry-independent molecules in the unit cell," Cryst. Growth Des. **8**, 2011–2018.

Brock, C. P. (**2016**). "High-Z' structures of organic molecules: their diversity and organizing principles," Acta Cryst. **B72**, 807–821.

Caruso, F., Raimondi, M. V., Daidone, G., Pettinari, C., and Rossi, M. (**2009**). "5-Amino-1-phenyl-3-trifluoromethyl-1*H*-pyrazole-4-carboxylic acid," Acta Crystallogr. Sect E. **65**, o2173–o2173.

Chatterjee, P., Dey, T., Pal, S., and Mukherjee, A. K. (**2017**). "Two mefenamic acid derivatives: structural study using powder X-ray diffraction, Hirshfeld surface and molecular electrostatic potential calculations," Z. Kristallogr. **232**, 385–394.

Das, D., Banerjee, R., Mondal, R., Howard, J. A. K., Boese, R., and Desiraju, G. R. (**2006**). "Synthon evolution and unit cell evolution during crystallisation. A study of symmetry-independent molecules (Z'>1) in crystals of some hydroxy compounds," Chem. Commun., 555–557.

Das, U., Chattopadhyay, B., Hazra, D. K., Sureshbabu, V. V., and Mukherjee, A. K. (**2016**). "Two carbamate derivatives with $Z' = 2$ and 3: an interplay of strong and weak hydrogen bonds," J. Mol. Str. **1122**, 290–298.

David, W. I. F., and Shankland, K. (**2008**). "Structure determination from powder diffraction data," Acta Crystallogr. A. **64**, 52–64.

Delley, B. (**1990**). "An all-electron numerical method for solving the local density functional for polyatomic molecules," J. Chem. Phys. **92**, 508–517.

Desiraju, G. R. (**2007**). "On the presence of multiple molecules in the crystal asymmetric unit (Z'>1)," CrystEngComm. **9**, 91–92.

Favre-Nicolin, V., and Cerný, R. (**2004**). "A better FOX: using flexible modelling and maximum likelihood to improve direct-space *ab initio* structure determination from powder diffraction," Z. Krist. - Cryst. Mat. **219**, 847–856.

Hao, X., Siegler, M. A., Parkin, S., and Brock, C. P. (**2005a**). "[M$(H_2O)_2$(15-crown-5)]$(NO_3)_2$: A system rich in polymorphic and modulated phases," Cryst.Growth Des. **5**, 2225–2232.

Hao, X., Chen, J., Cammers, A., Parkin, S., and Brock, C. P. (**2005b**). "A helical structure with $Z' = 10$," Acta Cryst. **B61**, 218–226.

Harris, K. D. M., and Cheung, E. Y. (**2004**). "How to determine structures when single crystals cannot be grown: opportunities for structure determination of molecular materials using powder diffraction data," Chem. Soc. Rev. **33**, 526.

Harris, K. D. M., Tremayne, M., and Kariuki, B. M. (**2001**). "Contemporary advances in the Use of powder X-Ray diffraction for structure determination," Angew. Chem. Int. Ed. **40**, 1626–1651.

Jelsch, C., Ejsmont, K., and Huder, L. (**2014**). "The enrichment ratio of atomic contacts in crystals, an indicator derived from the Hirshfeld surface analysis," IUCr J. **1**, 119–128.

Johnstone, R. D. L., Ieva, M., Lennie, A. R., McNab, H., Pidcock, E., Warren, J. E., and Parsons, S. (**2010**). "Pressure as a tool in crystal engineering: inducing a phase transition in a high-Z' structure," CrystEngComm. **12**, 2520–2523.

Larson, A. C., and Von Dreele, R. B. (**2000**). "General Structure Analysis System (GSAS), Los Alamos Laboratory Report, LAUR," 86–784.

Lee, C., Yang, W., and Parr, R. G. (**1988**). "Development of the colle-salvetti correlation-energy formula into a functional of the electron density," Phys. Rev. B. **37**, 785–789.

Lehmler, H.-J., Parlin, S., and Brock, C. P. (**2004**). "Packing conflicts in the $Z' = 5$ structure of $CF_3(CF_2)_3(CH_2)_{10}COOH$," Acta Cryst. **B60**, 325–332.

Lodochnikova, O. A., Startseav, V. A., Nikitana, L. E., Bodrov, A. V., Klimovitskii, A. E., Klimovitskii, E. N., and Litvinov, I. A. (**2014**). "When two symmetrically independent molecules must be different: "crystallization-induced diastereomerization" of chiral pinanyl sulfone," CrystEngComm. **16**, 4314–4321.

Martin, T., Fleissner, J., Milius, W., and Breu, J. (**2016**). "Behind crime scenes: the crystal structure of commercial luminol," Cryst. Growth Des. **16**, 3014–3018.

McKinnon, J. J., Jayatilaka, D., and Spackman, M. A. (**2007**). "Towards quantitative analysis of intermolecular interactions with Hirshfeld surfaces," Chem. Commun., 3814–3816.

Nichol, G. S., and Clegg, W. (**2006**). "The importance of weak C − H$\cdots$O bonds and $\pi\cdots\pi$ stacking interactions in the formation of organic 1,8-Bis(dimethylamino)naphthalene complexes with Z'>1," Cryst. Growth Des. **6**, 451–460.

Owczarzak, A. M., Samshuddin, S., Narayana, B., Yathirajan, H. S., and Kubicki, M. (**2013**). "Pseudosymmetry, polymorphism and weak interactions: 4,4′′-difluoro-5′-hydroxy-1,1′:3′,1′′-terphenyl-4′-carboxylic acid and its derivatives," CrystEngComm. **15**, 9893–9898.

Pagola, S., Stephens, P. W., Bohle, D. S., Kosar, A. D., and Madsen, S. K. (**2000**). "The structure of malaria pigment β-haematin," Nature. **404**, 307–310.

Perdew, J. P., Burke, K., and Ernzerhof, M. (**1996**). "Generalized gradient approximation made simple," Phys. Rev. Lett. **77**, 3865–3868.

Platteau, C., Lefebvre, J., Hemon, S., Baehtz, C., Danede, F., and Prevost, D. (**2005**). "Structure determination of forms I and II of phenobarbital from X-ray powder diffraction," Acta Cryst B. **61**, 80–88.

Politzer, P., and Murray, J. S. (**2015**). "Quantitative analyses of molecular surface electrostatic potentials in relation to hydrogen bonding and Co-crystallization," Cryst. Growth Des. **15**, 3767–3774.

Pramanik, S., Dey, T., and Mukherjee, A. K. (**2019**). "Five benzoic acid derivatives: crystallographic study using X-ray powder diffraction, electronic structure and molecular electrostatic potential calculation," J. Mol. Str. **1175**, 185–207.

Rehman, M. Z., Elsegood, M. R. J., Akbar, N., and Saleem, R. S. Z. (**2008**). "5-Amino-1-phenyl-1*H*-pyrazole-4-carboxylic acid," Acta Crystallogr. Sec E. **64**, 1312.

Rietveld, H. (**1967**). "Line profiles of neutron powder-diffraction peaks for structure refinement," Acta Crystallogr. **22**, 151–152.

Rohl, A. L., Moret, M., Kaminsky, W., Claborn, K., McKinnon, J. J., and Kahr, B. (**2008**). "Hirshfeld surfaces identify inadequacies in computations of intermolecular interactions in crystals: pentamorphic 1,8-dihydroxyanthraquinone," Cryst. Growth Des. **8**, 4517–4525.

Spackman, M. A., and McKinnon, J. J. (**2002**). "Fingerprinting intermolecular interactions in molecular crystals," CrystEngComm. **4**, 378–392.

Steed, K. M., and Steed, J. W. (**2015**). "Packing problems: high Z' crystal structures and their relationship to co-crystals, inclusion compounds, and polymorphism," Chem. Rev. **115**, 2895–2933.

Stewart, J. J. P. (**2007**). "Optimization of parameters for semiempirical methods V: modification of NDDO approximations and application to 70 elements," J. Mol. Model. **13**, 1173–1213.

Thompson, P., Cox, D. E., and Hastings, J. B. (**1987**). "Rietveld refinement of Debye-Scherrer synchrotron X-ray data from Al_2O_3," J. Appl. Crystallogr. **20**, 79–83.

Watts, A. E., Maruyoshi, K., Hughes, C. E., Brown, S. P., and Harris, K. D. M. (**2016**). "Combining the advantages of powder X-ray diffraction and NMR crystallography in structure determination of the pharmaceutical material cimetidine hydrochloride," Cryst.Growth Des. **16**, 1798–1804.

Wen, H.-L., Kang, J.-J., Dai, B., Deng, R.-H., and Hu. Chin, H.-W. (**2015**) "Syntheses, crystal structures and antibacterial activities of 5-chloro-3-m ethyl-1-phenyl-1H-pyrazole-4-carboxylic acid and its copper(II) compound," J. Struct. Chem. **34**, 33.

Werner, P. E., Eriksson, L., and Westdahl, M. (**1985**). "TREOR, a semi-ex-haustive trial-and-error powder indexing program for all symmetries," J. Appl. Cryst. **18**, 367–370.

Wolff, S. K., Grimwood, D. J., McKinnon, J. J., Turner, M. J., Jayatilaka, D., and Spackman, M. A. (**2012**). *Crystal Explorer 3.1* (University of Western Australia, Perth, Australia).